

# NARROWBAND INTERFERENCE REDUCTION TECHNIQUE IN IMPULSE RADIO (IR) UWB COMMUNICATION SYSTEM COEXISTING IN WPAN AND UNDERWATER ENVIRONMENT

**Bikramaditya Das<sup>1</sup>, Ch. Sasmita Das<sup>2</sup>, Susmita Das<sup>3</sup>, Bidyadhar Subudhi<sup>4</sup> and Bibhuti Bhusan Pati<sup>5</sup>**

<sup>1,5</sup>Department of Electrical Engineering, Veer Surendra Sai University of Technology, India  
E-mail: <sup>1</sup>adibik09@gmail.com and <sup>5</sup>pati\_bibhuti@rediffmail.com

<sup>2,3,4</sup>Department of Electrical Engineering, National Institute of Technology Rourkela, India  
E-mail: <sup>2</sup>ch.sasmitadas@gmail.com and <sup>4</sup>bidyadharnitrkl@gmail.com

## Abstract

The Impulse Radio based Ultra Wideband (IR-UWB) system transmits data by sending pulses, each with very small time duration followed by pauses that are approximately two hundred times that length. Rake receiver improves system performance by equalizing signals from different paths. This enables the use of Rake receiver techniques in UWB systems. For high data rate ultra-wideband communication system, performance comparison of ARake, PRake and SRake receivers are attempted. Although UWB communication offers a promising solution in an increasingly overcrowded frequency spectrum, mutual interference due to coexistence with other spectrally overlapping wireless system degrades the performance of both systems. The narrow band systems may cause interference with UWB devices as it is having very low transmission power and the large bandwidth. So it may jam the UWB receiver completely degrading their performance. Rake receiver alone fails to perform in such condition. A hybrid SRAKE-MMSE time domain equalizer is proposed to overcome this by taking into account both the effect of the number of rake fingers and equalizer taps. This scheme selects the first strongest multipath components and combines them using a SRake receiver based on the minimum mean square error (MMSE) criterion. It also combats inter-symbol interference by considering the same advantages. Study on non-line of sight indoor channel models illustrates that bit error rate performance of UWB SRAKE-MMSE (both LE and DFE types) improves for CM3 model with smaller spread compared to CM4 channel model cancelling out the narrowband interference. A modified UWB channel model is proposed using the Rician distribution for underwater communication. Again BER performance of the proposed receiver is compared with traditional receiver technique for the underwater UWB LOS channel model.

## Keywords:

RAKE-MMSE, LE, DFE, IEEE 802.15.3a, Underwater, NBI

## 1. INTRODUCTION

Ultra-wideband (UWB) radio is an emerging technology in WPAN wireless system that has attracted a great deal of interest from academia, industries, and global standardization bodies. The IEEE 802.15.3a (TG3a) and IEEE 802.15.4a (TG4a) are two task groups (TGs) within 802.15 working group (WG) that develop their standards based on UWB technology. UWB technology has been around since 1960, when it was mainly used for radar and military applications. Recent advances in silicon process and switching speeds are moving it into the commercial domain. One of the most promising commercial application areas for UWB technology is the very high data rate wireless connectivity of different home electronic devices at low cost and low power consumption. Ultra-wideband technology offers a solution for sharing the bandwidth resource and physical

size requirements of next-generation consumer electronic devices. In addition, UWB promises low susceptibility to multipath fading, high transmission security and simple design. A traditional UWB technology is based on single band systems employing carrier free or impulse radio communications. Impulse radio (IR) refers to the generation of a series of impulse like waveforms, each of duration in the hundreds of picoseconds [1], [2] and [7]. This type of transmission does not require the use of additional carrier modulation and is a baseband signal approach. UWB technology provides high data rate with low power spectral density due to modulation of extremely short pulses within 3.1 to 10.6 GHz [5]. The very low transmission power and the large bandwidth enable an UWB system to co-exist with narrowband communication [3] systems illustrated in Fig.1.

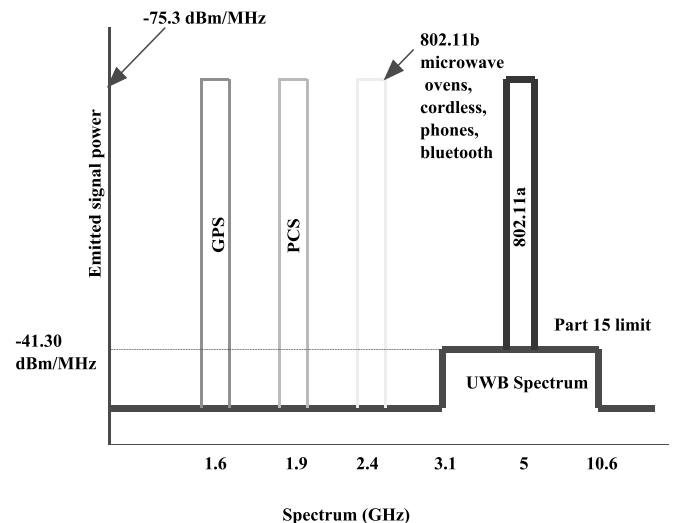


Fig.1. Spectrum of UWB and existing narrowband systems

Although UWB communication offers a promising solution in an increasingly overcrowded frequency spectrum, mutual interference due to coexistence with other spectrally overlapping wireless system degrades the performance of both systems [4]. The interference caused may jam the UWB receiver completely. According to Electromagnetic Compatibility (EMC) reports submitted to FCC [24], the narrowband interferences (NBI) expected by the UWB receivers are computer motherboard of emission level 42.7 dBm at 1.9 GHz, IEEE 802.11b at centre frequency 2.4 GHz, network interface card (NIC) of emission level 49.8 dBm at 3.75 GHz, LAN switch of 44.3 dBm at 3.75 GHz, peripheral component interconnect (PCI) card for a

personal computer 3.75 GHz and IEEE 802.11a (WLAN system) at centre frequency 5.25 GHz etc. [3]. Study of impact of NBI and suppression of NBI is one of the important issues associated with UWB applications [16], [18] and [19] and [12]. Performance enhancement by employing effective NBI mitigation techniques are discussed in this research work [20].

Section 2 introduces the principle of UWB Rake receiver considering its importance in UWB system. In section 3, UWB Rake receiver structure is analyzed in the presence of NBI. Simulation results for performance analysis of UWB Rake receiver and performance degradation of UWB SRake receiver in presence of NBI are presented in section 4 and 5 respectively. Section 6 explains the performance of UWB SRAKE-MMSE receiver and section 7 investigates the suppression of interference by using the same. Simulation results are presented in section 8. The conclusion is presented in section 9.

## 2. UWB RAKE RECEIVER STRUCTURE

The robustness of UWB signals to multipath fading [3] is due to their fine delay resolution, which leads to a high diversity order once combined with a Rake receiver. Rake receivers are used in time-hopping impulse radio systems and direct sequence spread spectrum systems for matched filtering of the received signal [2], [10] and [11]. The receiver structure consists of a matched filter that is matched to the transmitted waveform that represents one symbol and a tapped delay line that matches the channel impulse response [9] and [14]. It is also possible to implement this structure as a number of correlators that are sampled at the delays related to specific number of multipath components; each of those correlators is known as rake finger. Based upon the Rake receivers are three types. The All-Rake (ARake) receiver captures all most all the energy carried by a very large number of different multipath signals [8] and [13].

To reduce the rake complexity, a partial combining (called PRake) is used as partial combining of the energy, which combines the first arriving paths out of the available resolved multipath components. Selective combining (called SRake) is a suboptimum Rake receiver, which combines the energy selectively carried out by the strongest multipath components. A UWB Rake receiver structure is shown in Fig.2.

For a single user system, the continuous transmitted data stream is represented as [13]

$$s(t) = \sum_{k=-\infty}^{+\infty} d(k).p(t - kT_s) \tag{1}$$

where,  $d(k)$  are stationary uncorrelated BPSK data and  $T_s$  is the symbol duration. The UWB pulse  $p(t)$  has duration  $T_{uwb}$  ( $T_{uwb} < T_s$ ).

The channel impulse response is given by [6] and [22]

$$h(t) = \sum_{i=0}^M h_i \delta(t - \tau_i) \tag{2}$$

$M$  is the total number of paths in the channel. The received signal first passes through the receiver filter matched to the transmitted pulse and is given by,

$$\begin{aligned} r(t) &= s(t) * h(t) * p(-t) + n(t) * p(-t) \\ &= \sum_{k=-\infty}^{+\infty} d(k) \sum_i h_i m(t - kT_s - \tau_i) + \hat{n}(t) \end{aligned} \tag{3}$$

where,  $p(-t)$  represents the receiver matched filter and  $n(t)$  is the Additive White Gaussian Noise (AWGN) with zero mean and variance  $N_0/2$ . Also,

$$m(t) = p(t) * p(-t) \text{ and } \hat{n}(t) = n(t) * p(-t)$$

Combining the channel response with the transmitter pulse shape and the matched filter,

$$\tilde{h}(t) = p(t) * h(t) * p(-t) = \sum_{i=0}^M h_i m(t - \tau_i). \tag{4}$$

The received signal sampled at the  $l^{\text{th}}$  rake finger in the  $n^{\text{th}}$  data symbol interval is given by,

$$v(nT_s + \tau'_l + t_0) = \sum_{k=-\infty}^{+\infty} \tilde{h}((n-k)T_s + \tau'_l + t_0).d(k) \tag{5}$$

where,  $\tau'_l$  is the delay time corresponding to the  $l^{\text{th}}$  rake finger and is an integer multiple of  $T_m$ . Parameter  $t_0$  corresponds to a time offset and is used to obtain the best sampling time. For the following analysis  $t_0$  will be set to zero. The Rake combiner output at time  $t = n.T_s$  is,

$$y[n] = \sum_{l=1}^L \beta_l.v(nT_s + \tau'_l) + \sum_{l=1}^L \beta_l.\hat{n}(nT_s + \tau'_l). \tag{6}$$

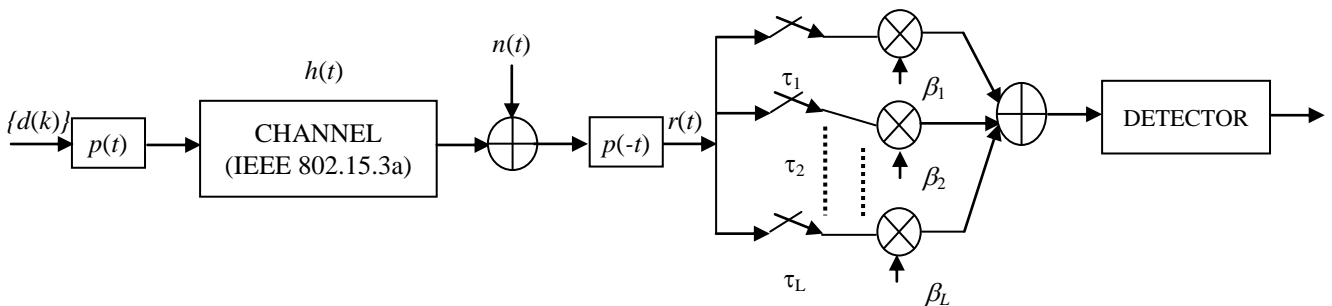


Fig.2. UWB Rake receiver structure

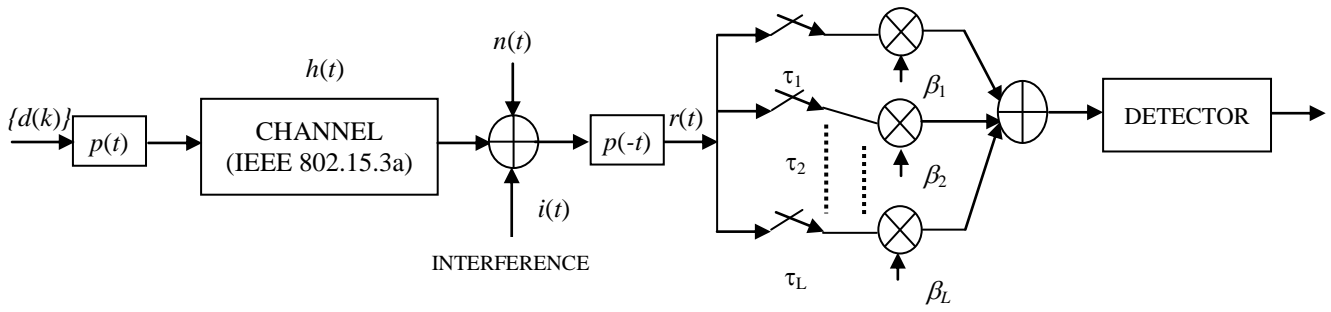


Fig.3. UWB Rake receiver model in presence of NBI

### 3. UWB SRAKE RECEIVER IN PRESENCE OF NBI

The working of UWB system in co-existence with other narrowband systems over their large bandwidth is challenging [12]. Thus, UWB systems must cope with these narrow band interference (NBI) using their high processing gain. However, due to very low transmission power, it is not sufficient to suppress high levels of NBI are typically from nearby narrowband radio systems using a bandwidth of up to a few MHz. In many cases, the power of NBI is a few tens of dBs higher than both the signal and noise power. The narrowband interference (NBI) signal is modelled as a traditional single carrier BPSK modulated waveform, given by [14] and [16]

$$i(t) = \sqrt{2P_1} \cos(\omega_0 t + \theta) \sum_{p=-\infty}^{\infty} g_k z(t - kT_1 - \tau_1) \quad (7)$$

where,  $P_1$  is average transmit power of the narrowband waveform.  $\omega_0 = 2\pi f_0$  is carrier frequency of the narrowband waveform.  $\theta$  is the random phase of the carrier.  $\{g_k\}$  are the randomly modulated BPSK symbols where  $g_k \in \{\pm 1\}$ ,  $T_1$  is the symbol period,  $\tau_1$  is a random delay uniformly distributed in  $[0, T_1]$  and  $z(t)$  is the baseband wave form shape. UWB Rake receiver model considering NBI is shown in Fig.3.

The received signal passes through the receiver filter matched is given by [14]

$$r(t) = A(t) * h(t) * p(-t) + n(t) * p(-t) + i(t) * p(-t) \quad (8)$$

Interference coexisting with the same system generates extra signal which can't be easily detected at the output. Rather by coexisting with original pulse, it will decrease the performance of receiver. If such interference is not properly suppressed, then this will jam the receiver and the system performance degrades [12].

### 4. PERFORMANCE ANALYSIS OF RAKE RECEIVERS IN IR-UWB SYSTEM

BER performance of Rake receiver in IR-UWB system is observed through MATLAB simulation. Performance comparison among ARake, SRake, and PRake receiver is carried out using different IEEE UWB channel models [6] as shown in Fig.4. ARake receiver provides better result than other two types of Rake. Since a UWB signal has a very wide bandwidth, ARake receiver combining all the paths of the incoming signal is practically unfeasible. Therefore, SRake becomes the practical

choice. It is observed from Fig.4(a) that using the perfect channel impulse response and estimating 8 number of rake fingers; ARake provides best performance of gaining more than 4dB SNR over the PRake receiver at  $BER = 10^{-3}$ . It is also found that SRake and PRake have almost the same diversity order, and differs by less than 2dB due to line of sight (LOS) channel medium.

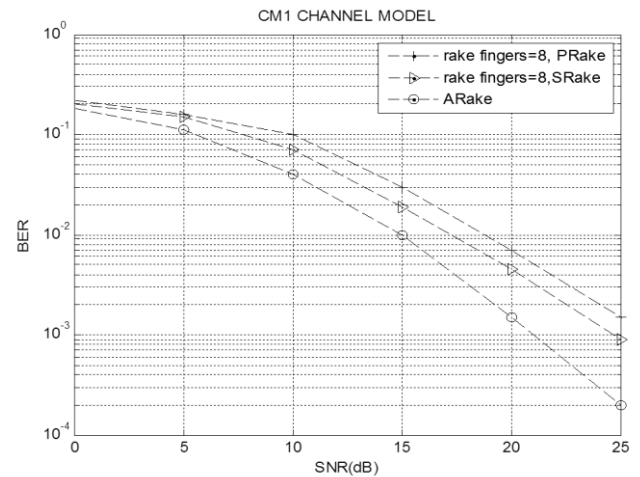


Fig.4(a). BER performance of Rake receivers for CM1 model

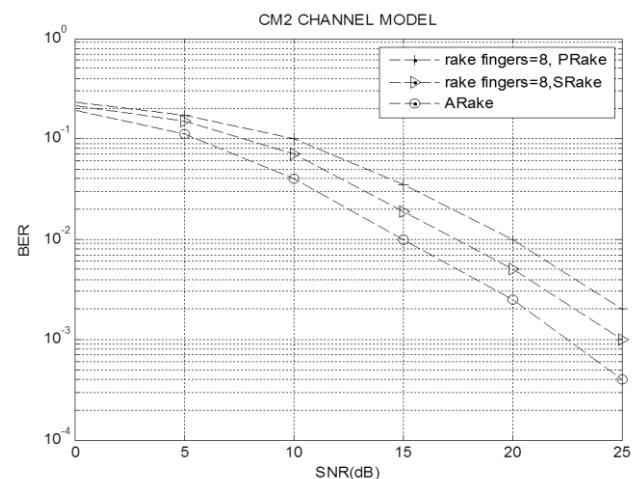


Fig.4(b). BER performance of Rake receivers for CM2 model

In the analysis CM2 channel model, SRake performance approaches almost the same performance level as ARake. SRake receiver provides 3dB SNR improvement at  $10^{-2}$  BER floor over the PRake as shown in Fig.4(b).

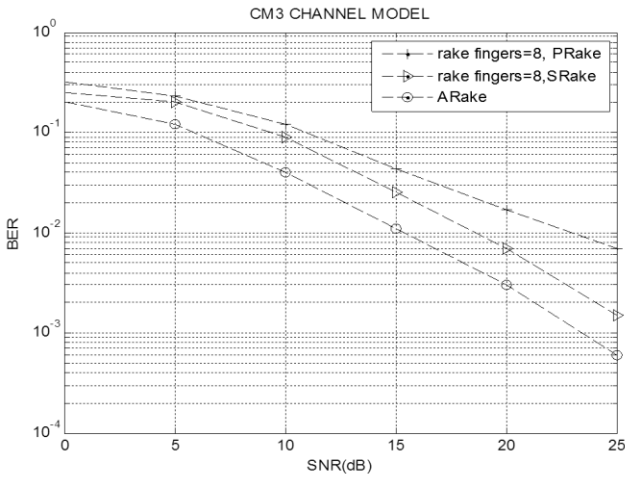


Fig.4(c). BER performance of Rake receivers for CM3 model

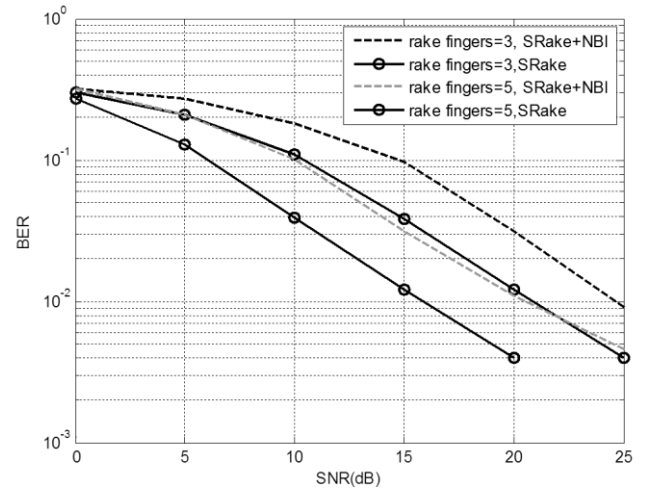


Fig.5. Performance of SRake receiver for CM1 channel model

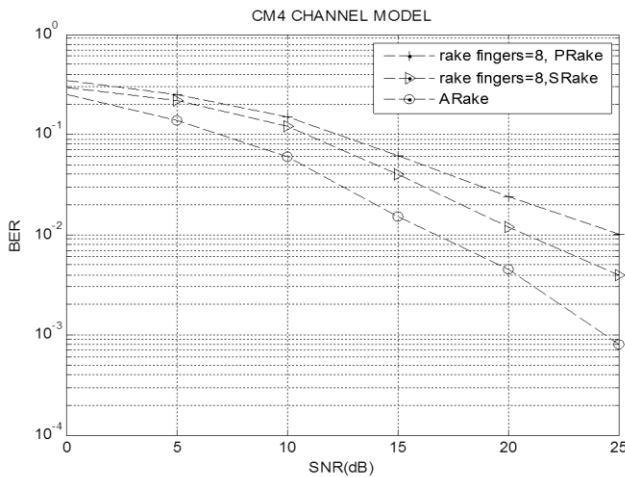


Fig.4(d). BER performance of Rake receivers for CM4 model

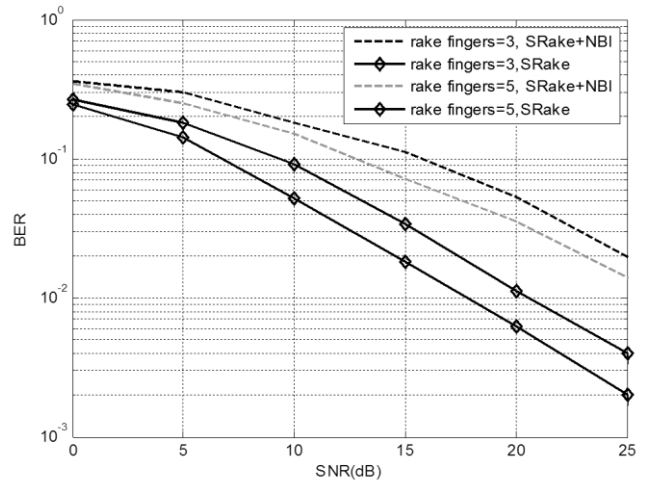


Fig.6. Performance of SRake receiver for CM2 channel model

In Fig.4(c) showing SRake receiver performance, gain of more than 4dB SNR over the PRake at BER=10<sup>-2</sup> for NLOS CM3 channel environment. Using CM4 channel model, for the same simulation parameter SRake performs better as shown in Fig.4(d). A SNR gain of more than 5dB is observed on 10<sup>-2</sup> BER floor for SRake. At low SNR's the system noise is more and hence the system degradation is noticed. More signal energy capture is required to overcome it. This can be achieved by increasing the numbers of rake fingers in Rake receiver structure.

### 5. STUDY OF PERFORMANCE DEGRADATION OF UWB SYSTEM IN PRESENCE OF NBI

SRake receiver in UWB system performance in absence and presence of NBI is studied and found that NBI deteriorates the system performance. In this study SRake with both 3 and 5 rake fingers is considered. An NBI with signal to interference ratio (SIR) of -20dB is added to the UWB channel model.

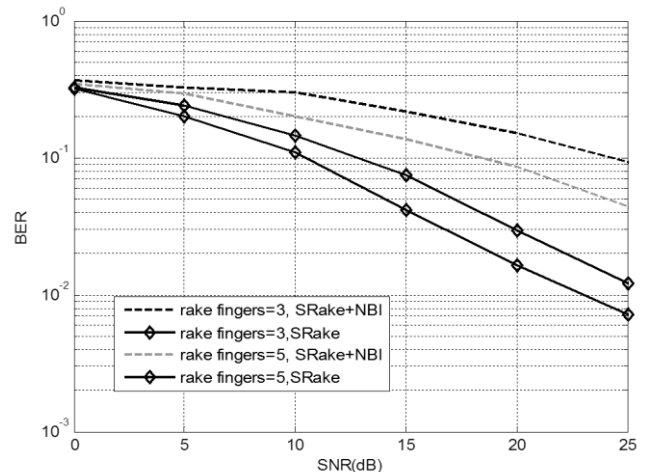


Fig.7. Performance of SRake receiver for CM3 channel model

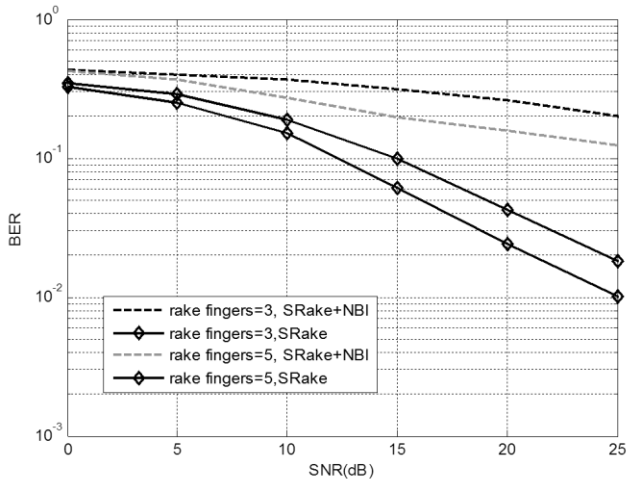


Fig.8. Performance of SRake receiver for CM4 channel model

However, as discussed before with increase in rake fingers the performance of SRake receiver increases. When the number of rake fingers is increased to 5, similar degradation in performance is noticed in both CM1 LOS channel medium and in CM2 NLOS channel medium as shown in Fig.6. As shown in Fig.7 for CM3 channel model, at SNR=20dB, UWB SRake receiver bit error rate (BER) passes from  $1.2 \times 10^{-2}$  to  $0.95 \times 10^{-2}$  for 3 number of rake fingers and from  $0.7 \times 10^{-2}$  to  $0.44 \times 10^{-1}$  for 5 number of rake fingers under the effect of NBI. The performance of SRake receiver in presence of NBI is almost flat above  $10^{-1}$  BER floor. The receiver structure cannot and hence deteriorates. So it is concluded as the multipath is reasonably high for CM3 and CM4 channel models, Rake receiver structure performance fails to eliminate NBI alone.

## 6. UWB SRAKE-MMSE RECEIVER STRUCTURE

This was achieved using Eigen value decomposition model for a hybrid SRAKE-MMSE receiver structure for high data rate UWB system is studied by the advantages of both rake fingers and equalizer taps. A major advantage of MMSE scheme relative to other interference suppression scheme is that explicit knowledge of interference parameter is not required [15] and [16].

The receiver structure is illustrated in Fig.9 and consists in a SRake receiver followed by a linear MMSE equalizer. The received signal first passes through the receiver filter matched to the transmitted pulse. The output of the receiver filter is sampled at each rake finger [14]. The minimum rake finger separation is  $T_m = T_s / N_u$ , where  $N_u$  is chosen as the largest integer value that would result in  $T_m$  spaced uncorrelated noise samples at the rake fingers. For general selection combining, the rake fingers ( $\beta$ 's) are selected as the largest  $L$  ( $L \leq N_u$ ) sampled signal at the matched filter output within one symbol time period at time instants  $\tau'_l$ ,  $l = 1, 2, \dots, L$ .

For a minimum mean square error (MMSE) SRake receiver, the conventional finger selection algorithm is to choose the paths with highest signal-to-interference-plus-noise ratios (SINRs) [17].

The noiseless received signal is given by Eq.(5). As derived in section 2, Rake combiner output at time  $t = n.T_s$  is

$$y[n] = \sum_{l=1}^L \beta_l \cdot v(n.T_s + \tau'_l) + \sum_{l=1}^L \beta_l \cdot \hat{n}(n.T_s + \tau'_l) \quad (9)$$

Assuming that the  $n$ th data bit is being detected, the MMSE criterion consists in minimizing

$$E \left[ \left| d(n) - \hat{d}(n) \right|^2 \right] \quad (10)$$

where,  $\hat{d}(n)$  is the equalizer output. From the Rake output signal, the desired signal, the undesired ISI and the noise are distinguished as,

$$y(n) = \left[ \sum_{l=1}^L \beta_l \tilde{h}(\tau'_l) \right] \cdot d(n) + \sum_{k \neq n} \sum_{l=1}^L \beta_l \tilde{h}((n-k).T_s + \tau'_l) \cdot d(k) + \sum_{l=1}^L \beta_l \hat{n}(n.T_s + \tau'_l) \quad (11)$$

where, the first term represents the desired output. The noise samples at different fingers,  $\hat{n}(n.T_s + \tau'_l)$ ,  $l = 1 \dots L$ , are uncorrelated and therefore independent, since the samples are taken at approximately the multiples of the inverse of the matched filter bandwidth. It is assumed that the channel has a length of  $(n_1 + n_2 + 1).T_s$ . That is, there is pre-cursor ISI from the subsequent  $n_1$  symbols and post-cursor ISI from the previous  $n_2$  symbols, and  $n_1$  and  $n_2$  are chosen large enough to include the majority of the ISI effect [21] and [23]. Using Eq.(11), the Rake output can be expressed now in a simple form as,

$$y(n) = \alpha_0 \cdot d(n) + \sum_{\substack{k=-n_1 \\ k \neq 0}}^{n_2} \alpha_k \cdot d(n-k) + \tilde{n}(n) = \phi^T [n] + \tilde{n}(n) \quad (12)$$

where  $\phi = [\alpha_{n_1} \dots \alpha_0 \dots \alpha_{n_2}]$  and  $d[n] = [d(n+n_1) \dots d(n) \dots d(n-n_2)]^T$ .

Coefficient of  $\alpha_k$ 's are obtained by matching Eq.(11) and Eq.(12). The noise at Rake output is  $\tilde{n}(n) = \sum_{l=1}^L \beta_l \hat{n}(n.T_s + \tau'_l)$ .

The output of the linear equalizer (LE) is obtained as

$$\hat{d}(n) = \sum_{r=-k_1}^{k_2} c_r \cdot y(n-r) = c^T \gamma(n) + c^T \eta(n) \quad (13)$$

where  $c = [c_{K_1} \dots c_0 \dots c_{K_2}]$  contains the equalizer taps. Also

$$\gamma[n] = [\phi^T d[n+k_1] \dots \phi^T d[n] \dots \phi^T d[n-k_2]]^T \quad (14)$$

$$\eta[n] = \left[ \tilde{n}(n+K_1) \dots \tilde{n}(n) \dots \tilde{n}(n-K_2) \right]^T \quad (15)$$

The mean square error (MSE) of the equalizer,

$$E \left[ \left| d(n) - c^T \gamma[n] - c^T \eta[n] \right|^2 \right] \quad (16)$$

Eq.(16) is a quadratic function of the vector  $c$ , has a unique minimum solution. Defining matrices  $R$ ,  $p$  and  $N$  as,

$$R = E[\gamma[n] \cdot \gamma^T [n]] \quad (17)$$

$$p = E[d(n) \cdot \gamma[n]] \quad (18)$$

$$N = E[\eta[n] \cdot \eta^T [n]] \quad (19)$$

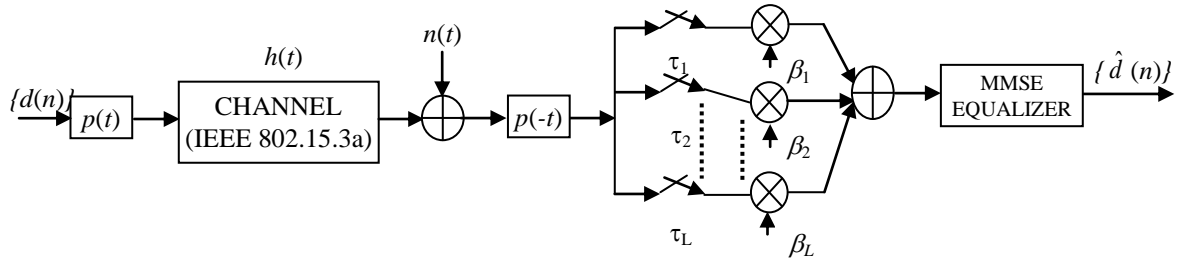


Fig.9. UWB SRAKE-MMSE receiver structure

The equalizer taps are given by

$$c = (R+N)^{-1} \cdot p \tag{20}$$

and the MMSE is

$$J_{\min} = \sigma_d^2 - p^T (R + N)^{-1} \cdot p \tag{21}$$

$$\sigma_d^2 = E[d(n)]^2$$

This Rake equalizer receiver will eliminate ISI as far as the number of equalizer's taps gives the degree of freedom required.

The equalizer output can be expressed as,

$$\hat{d}(n) = q_0 \cdot d(n) + \sum_{i=0}^{L-1} q_i \cdot d(n-i) + w(n) \tag{22}$$

with  $q_n = \alpha_n \cdot c_n$

The variance of  $w(n)$  is,

$$\sigma_{w(n)}^2 = \left( \sum_{i=-K_1}^{K_2} c_i^2 \right) \left( \sum_{i=1}^L \beta_i^2 \right) \cdot E_p \cdot N_0 / 2 \tag{23}$$

where  $E_p$  is the pulse energy. In the case of decision feedback equalizer (DFE), assuming error free feedback, the input data vector can be written in the form of

$$\gamma_{DFE}[n] = [\Phi^T d[n+k_1] \dots \Phi^T d[n] d[n-1] \dots d[n-k_2]] \tag{24}$$

### 7. UWB SRAKE-MMSE RECEIVER IN PRESENCE OF NBI

A narrow band interference model, that is generally WLAN, which coexists with UWB signal at the frequency 5.25 GHz as, provided in Eq.(7). The received signal sampled at the  $l$ th rake finger in the  $n$ th data symbol interval given by Eq.(7). The Rake combiner output [14] at time  $t = n.T_s$

$$y[n] = \sum_{i=1}^L \beta_i \cdot v(n.T_s + \tau_i) + \sum_{i=1}^L \beta_i \cdot i(n.T_s + \tau_i) + \sum_{i=1}^L \beta_i \cdot \hat{n}(n.T_s + \tau_i) \tag{25}$$

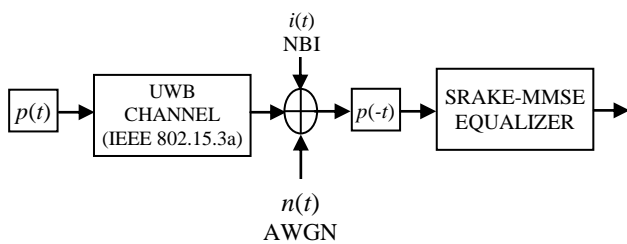


Fig.10. UWB RAKE-MMSE receiver structure with NBI

The received signal is sampled at pulse repetition frequency after passing through the correlation receiver. The samples are linearly combined using the MMSE criterion, so that weights are effective to suppress the NBI [16]. The MMSE weight vector  $c^*$  is given by

$$c^* = (R_s + R_I + R_N)^{-1} \cdot p \tag{26}$$

where  $R_s$ ,  $R_I$ ,  $R_N$  are the autocorrelation of the signal, the NBI and the noise respectively. So The MMSE can be mathematically expressed as

$$J_{\min} = \sigma_d^2 - p^T (R_s + R_I + R_N)^{-1} \cdot p \tag{27}$$

$$\sigma_d^2 = E[d(n)]^2 \tag{28}$$

Thus, it is concluded that in the NBI suppression analysis using SRAKE-MMSE receiver, the correlation between the samples of the received signal plays the main role. Assuming  $n(t)$  is not correlated to  $i(t)$  and has an impulsive auto-correlation, Hence the NBI is modelled as single tone.

## 8. SIMULATION STUDY AND RESULTS

### 8.1 PERFORMANCE ANALYSIS OF SRAKE-MMSE RECEIVER IN UWB SYSTEM

Performance of hybrid SRAKE-MMSE equalizer receiver for high data rate UWB system is investigated through MATLAB simulation. In the evaluation of receiver performance, high multipath UWB propagation channel models, i.e. CM3 and CM4 are considered. In UWB SRAKE-MMSE receiver design, selection of the number of rake fingers and the length of equalizer taps play a main role. The rake fingers are regularly positioned according to time channel spread and the number of fingers [17].

The pulse shape adopted in the simulation study is taken as the second derivative of the Gaussian pulse with pulse width 0.35 nsec. The root raised cosine (RRC) pulse with roll off factor  $\alpha = 0.5$  is used in the pulse-shaping filter. An oversampling factor of eight is used for the root raised cosine (RRC) pulse. According to this sampling rate, time channel spread is chosen equal to 100 for CM4 and 70 for CM3, this corresponds to respectively  $12 = 100/8$  and  $9 = 70/8$  transmitted symbols. This choice enables to gather 99% of the channel energy. The coherence bandwidths of CM3 and CM4 simulation are 10.6 MHz and 5.9 MHz respectively. The data rate is chosen to be 200 Mbps resulting in symbol duration of 5 nsec. The simulation is performed at 100.8 GHz sampling rate. The rake finger minimum time spacing is chosen as 0.1786 nsec, for  $N_u = 28$ .

Each channel is normalized prior to multiplying it by the shadowing factor. The shadowing factor is also normalized to have unit average value over all the 100 channel realizations. The transmitter pulse shape has unit energy. The size of the transmitted packets is equal to 2560 BPSK symbols including a training sequence of length 500. CIR remains constant over the time duration of packet. Table.1 provides all the simulation parameter used for SRAKE-MMSE receiver. Performance of UWB SRAKE-MMSE receiver varying length of equalizer taps and rake fingers for CM3 and CM4 as shown in Fig.11 and 12.

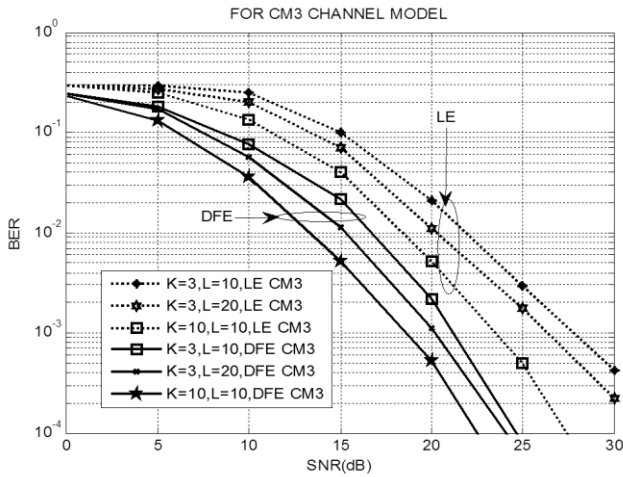


Fig.11. Performance of UWB SRAKE-MMSE-receiver for different length of equalizer taps and rake fingers for CM3 channel model

Fig.11 shows that keeping the number of rake fingers constant ( $K=3$ ), almost 1dB SNR gain at a BER level of  $10^{-3}$  is observed with increase in length of equalizer taps from  $L=10$  to 20. Whereas keeping the number of equalizer taps same ( $L=10$ ), around 4dB SNR improvement is obtained increasing the rake fingers from  $K=3$  to 10. Further decision feedback equalizer (DFE) provides more than 5dB SNR improvement than that of linear equalizer (LE) for  $K = 10, L = 10$  in case of CM3 channel model.

Table.1. Simulation Parameter for SRAKE-MMSE receiver

Parameter	Values
Data rate	200 Mbps
Pulse width	0.35 ns
Symbol duration	5ns
Pulse energy	1
$T_m$	0.1786 ns
$N_u$	28
Channel spread	CM3=70, CM4=100
Pilot carrier	500

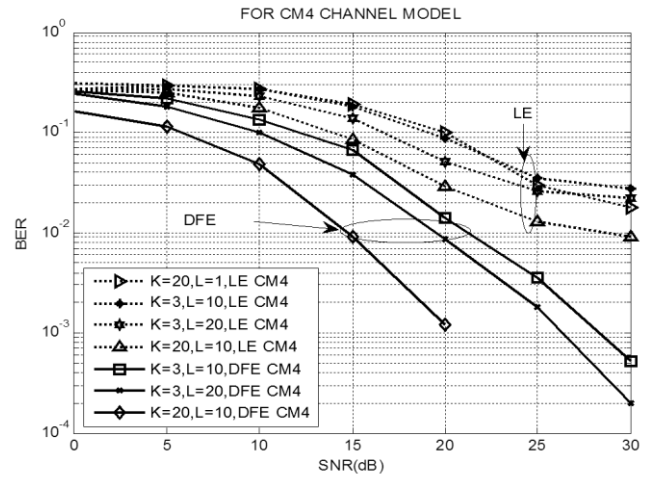


Fig.12. Performance of UWB SRAKE-MMSE-receiver for different length of equalizer taps and rake fingers for CM4 channel model

The performance improvement is noticeable when the number of rake fingers and the equalizer taps are simultaneously increased to  $K = 20$  and  $L = 10$  as shown in Fig.12. Comparing the BER performances, it is observed that on different UWB NLOS channel models (CM3 and CM4) LE fails to perform satisfactorily at high SNR's due to presence of zeros outside the unit circle. These difficulties are overcome by using DFE of same filter length. A DFE outperforms a linear equalizer of the same filter length, and the performance further improves with more equalizer tap length. At high SNR's, ISI affects the system performance, where at low SNR's the system noise degrades the performance. So receiver with more number of rake fingers outperforms the one that has more equalizer taps at high SNR condition.

## 8.2 PERFORMANCE ANALYSIS OF SRAKE-MMSE RECEIVERS FOR NBI MITIGATION IN UWB SYSTEM

It is already studied in section 5 that UWB system performance degrades due to interferers from narrowband system. If NBI is not suppressed, the receiver may be jammed also. For suppression of NBI, the SRAKE-MMSE receiver structure is studied using the same UWB channel models. The simulation is analyzed using SRake with 5 fingers and number of equalizer taps are 20 and an NBI with a SIR=-20dB. The parameters are set as discussed in section 8.

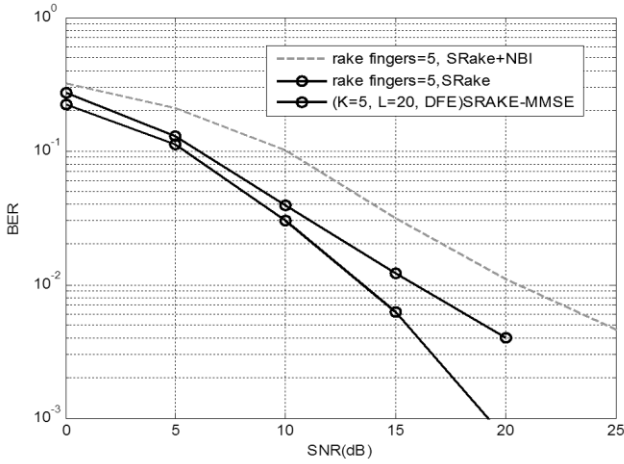


Fig.13. Performance of SRAKE-MMSE receiver with NBI for CM1 channel model

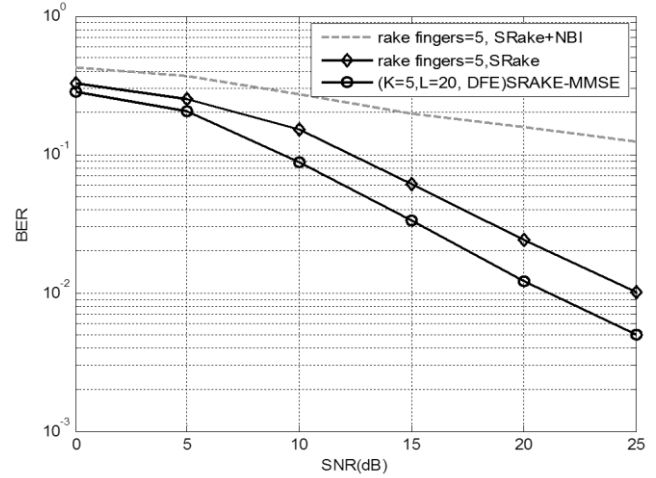


Fig.16. Performance of SRAKE-MMSE receiver with NBI for CM4 channel model

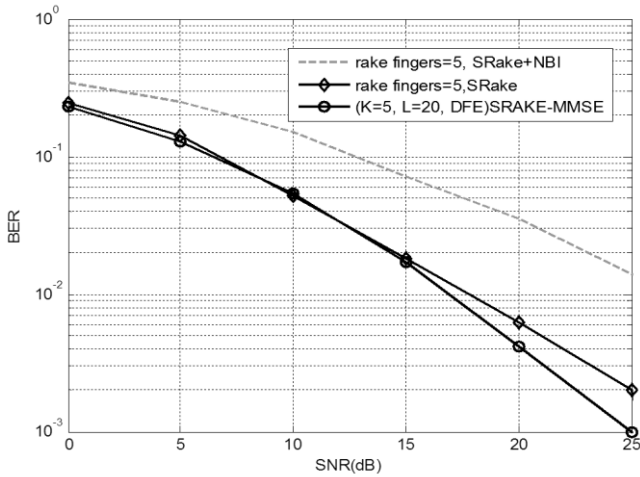


Fig.14. Performance of SRAKE-MMSE receiver with NBI for CM2 channel model

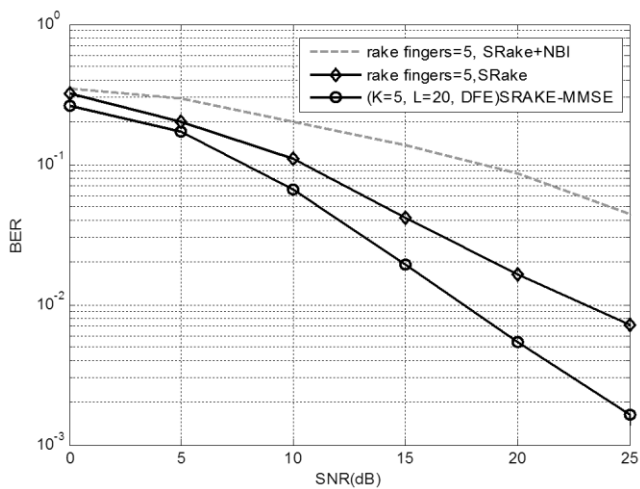


Fig.15. Performance of SRAKE-MMSE receiver with NBI for CM3 channel model

Similar effects in performance are observed for CM3 and CM4 models also. Table.2 describes the improvement in BER level at SNR =20dB.

Table.2. Improvement in BER level at SNR=20dB

Receiver structure	UWB SRAKE-MMSE Receiver in presence of NBI (SIR=-20dB)	UWB SRake receive in presence of NBI (SIR=-20dB)
UWB Channel models	BER	BER
CM1	$\ll 0.1 \times 10^{-2}$	$0.11 \times 10^{-1}$
CM2	$0.4 \times 10^{-2}$	$0.36 \times 10^{-1}$
CM3	$0.5 \times 10^{-2}$	$0.88 \times 10^{-1}$
CM4	$0.12 \times 10^{-1}$	$0.155 \times 10^0$

### 8.3 PERFORMANCE ANALYSIS OF SRAKE-MMSE RECEIVERS FOR NBI MITIGATION IN UNDERWATER MODIFIED UWB CHANNEL MODEL

The speed of sound underwater is approximately 1500 m/s, which provides a large propagation delays and motion-induced Doppler effects. Phase and amplitude fluctuations may induce high bit error probability. Interference is another phenomenon in underwater acoustic networks, causing frequency-selective fading in underwater channels. Research are carried out assuming Rayleigh fading in nature, but it is observed that Rayleigh fading exhibits better in terrestrial communication than UWA communication [25]. According to Ray theory, the number of Eigen rays reaching the receiver must be a Poisson distribution with a mean value. A modified UWB S-V channel model for underwater acoustic networks is proposed. In an underwater acoustic channel, the communication frequency range is inferior to 10 kHz. In short-range transmission, the carrier frequency is 550 Hz in shallow water and 2 kHz in deep water. The carrier frequency for long-range transmission is 1500 Hz. In all cases, the fractional bandwidth  $(fH - fL)/((fH + fL)/2)$



is much greater than 0.20–0.25. Therefore, the underwater acoustic channel can be modeled as a UWB channel (IEEE 802.15.3a). The S-V model is having two Poisson models, employed in the modeling of the path arrivals in UWB communications. The two Poisson models are for the first path of each path cluster and for the paths or rays within each cluster respectively. Applying the S-V model into underwater acoustic channels, the arrival of clusters is modeled as a Poisson arrival process with rate  $\Lambda$ , whereas, within each cluster, subsequent multipath contributions or rays also arrive according to a Poisson process. The distributions of the cluster arrival time and the ray arrival time are given by [6]. It is desired to model the multipath channel gain as a Rician distribution as per the above discussion. According to Eq.(29), the average power decay profile is characterized by an exponential decay of the amplitude of the clusters and a different exponential decay for the amplitude of the received pulses within each cluster. In underwater S-V model, the gain of the  $k^{th}$  path within the  $l$ th cluster is a complex random value with a modulus  $\beta_{kl}$  and a phase  $\theta_{kl}$ . It is assumed that the  $\beta_{kl}$  values in an underwater acoustic channel are statistically independent and are Rician-distributed positive random variables, whereas the  $\theta_{kl}$  values are assumed to be statistically independent uniform random variables over  $[0, 2\pi]$  [26].

$$\beta_{kl}^{-2} = \beta_{ool}^{-2} \exp\left(\frac{-T_l}{\Gamma}\right) \exp\left(\frac{-\tau_{kl}}{\gamma}\right) \quad (29)$$

where the term  $\beta_{ool}$  represents the average energy of the first path of the first cluster, whereas  $\Gamma$  and  $\gamma$  are the power decay coefficients for clusters and multipath, respectively. Using the experimental data of [26], the modified channel model can used to transfer data by using the proposed SRAKE-MMSE receiver with narrowband interference technique in LOS medium as shown in Fig.17. The BER performance of SRAKE-MMSE receiver with the effect of NBI in modified underwater LOS channel model is compared with SRake receiver and found to be better at both low and high SNR. But the application of the proposed receiver in NLOS modified underwater UWB channel model is still challenging.

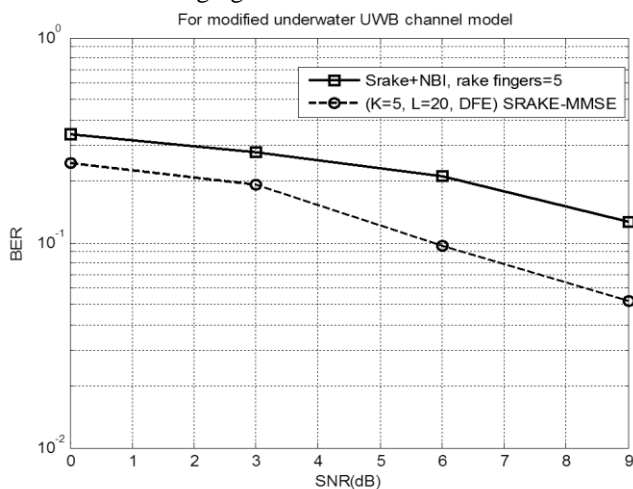


Fig.17. Performance of SRAKE-MMSE receiver with NBI for CM1 channel model in modified Underwater UWB channel model

## 9. CONCLUSION

IR-UWB is an emerging as a solution for the IEEE 802.15a (TG3a) standard, which provides low complexity, low cost, low power consumption and high data-rate in Wireless Personal Area Network (WPAN) system. For high data rate and short range, the receiver combats NBI interference by taking advantage of the Rake receiver and MMSE equalizer structure. MMSE equalizer operating at low to medium SNR's, the number of rake fingers is the dominant factor to improve system performance, while at high SNR's the number of equalizer taps plays a significant role. From this study, it can be concluded that UWB SRAKE-MMSE receiver is effectively robust against the NBI by taking the benefit of rake finger and equalizer taps. For the modified UWB underwater channel, the performance of proposed technique is decreased due to large propagation delays and motion-induced Doppler effects. From implementation point of view, the proposed narrowband interference suppression technique based upon SRake followed by MMSE equalizer is costly and more complex applied in DSP processor and acoustic underwater vehicles (AUV) communication. So designing an efficient scheme without increasing the system complexity to mitigate strong interferences has been the major focus of this research work.

## REFERENCES

- [1] Moe Z. Win and Robert A. Scholtz, "Impulse Radio--How it Works," *IEEE Communications Letters*, Vol. 2, No. 2, pp.36-38, 1998.
- [2] Moe Z. Win and Robert A. Scholtz, "Ultra-wide bandwidth time hopping spread-spectrum impulse radio for wireless multiple access communications," *IEEE Transactions on Communications*, Vol. 48, No. 4, pp.679-689, 2000.
- [3] J. R. Foerster, "The Effects of Multipath Interference on the Performance of UWB Systems in an Indoor Wireless Channel," *53rd IEEE VTS Vehicular Technology Conference*, Vol. 2, No. 69, pp.1176-1180, 2001.
- [4] Li Zhao, A. M. Haimovich, and H. Grebel, "Performance of ultra-wideband communications in the presence of interference," *IEEE proceedings of International Conference on Communication*, Vol. 1, pp.2948-2952, 2001.
- [5] Federal Communications Commission, Revision of part 15 of the commission's rules regarding ultra-wideband transmission systems, first report and order (ET Docket 98-153), Adopted Feb. 14, 2002, Released Apr. 22, 2002.
- [6] J. Foerster and Q. Li, "Channel modeling subcommittee report final", *IEEE P802.15 WG for WPANs Technical Report*, No. 02/490r0-SG3a, 2002.
- [7] JFM Gerrits and JR.Farserotu, "Wavelet generation circuit for UWB impulse radio applications," *IEEE Electronics Letters*, Vol. 38, No. 25, pp.1737-1738, 2002.
- [8] D. Cassioli, Moe Z. Win, F. Vatalaro and A.F. Molisch, "Performance of low-complexity RAKE reception in a Realistic UWB channel," *IEEE International Conference on Communication*, Vol. 2, pp. 763-767, 2002.
- [9] J. D. Choi and W. E. Stark, "Performance of ultra-wideband communications with suboptimal receivers in

- multipath channels," *IEEE Journal on Selected Areas in Communications*, Vol. 20, No. 9, pp.1754-1766, 2002.
- [10] J. D. Choi and W. E. Stark, "Performance of ultra-wideband communications with suboptimal receivers in multipath channels," *IEEE Journal on Selected Areas in Communications*, Vol. 20, No. 9, pp.1754-1766, 2002.
- [11] J. Foerster, "The Performance of a Direct-Sequence Spread Ultra-Wideband System in the Presence of Multipath, Narrowband Interference and Multiuser Interference," *IEEE Conference on Ultra Wideband Systems and Technologies*, pp.87-92, 2002.
- [12] J.R. Foerster, "Interference modelling of pulse-based UWB waveforms on narrowband systems," *IEEE 55th Vehicular Technology Conference*, Vol. 4, pp.1931-1935, 2002.
- [13] Rajeswaran, V.S. Somayazulu, and J.R. Foerster, "Rake performance for a pulse based UWB system in a realistic UWB indoor channel," *IEEE International Conference on Communications*, Vol.4, pp.2879-2883, 2003.
- [14] N. Boubaker and K.B. Letaief, "A Low Complexity RAKE Receiver in a realistic UWB Channel and in the presence of NBI," *IEEE Wireless Communications and Networking*, Vol. 1, pp.233-237, 2003.
- [15] S. Gezici, H. V. Poor and H. Kobayashi, "Optimal and Suboptimal Finger Selection Algorithms for MMSE Rake Receivers in Impulse Radio Ultra-Wideband Systems," *IEEE Wireless Communications and Networking Conference*, Vol. 2, pp.861-866, 2004.
- [16] Zhao Guannan, Jin Minglu and Fan Wei, "A Low-complexity NBI Suppression Algorithm in UWB Systems," pp.1-4, 2006.
- [17] Thomas Zasowski and Armin Wittneben, "UWB transmitted reference receivers in the presence of co-channel interference," *IEEE 17th International Symposium on Personal, Indoor and Mobile Radio Communications*, pp. 1-5, 2006.
- [18] M.K Lakshmanan and H. Nikoogar, "Mitigation of interference from wideband IEEE 802.11a source on UWB wireless communication using frequency selective wavelet packets," *IEEE International conference on waveform diversity and design*, pp.50-54, 2007.
- [19] Huy Quach and Anh Dinh, "Narrowband interference elimination in UWB communications systems," *Canadian Conference on Electrical and Computer Engineering*, pp. 1341 - 1344, 2007.
- [20] Y. Wang and X. Dong, "Spectrum shaping and NBI suppression in UWB communications," *IEEE Transactions on Wireless Communications*, Vol.6, No.5 pp.1944-1952, 2007.
- [21] F. Triesch and A. Wittneben, "MLSE post-detection for ISI mitigation and synchronization in UWB Low Complexity Receivers," *IEEE 65th Vehicular Technology Conference*, pp. 2915 - 2919, 2007.
- [22] C. Ramesh and V. Vaidehi, "Performance Analysis of UWB Channels for Wireless Personal Area Network," *Wireless Personal Communication, Springer*, Vol. 41, No. 2, pp. 169-178, 2007.
- [23] Xudong Ma, "Reduced Complexity Demodulation and Equalization Scheme for Differential Impulse Radio UWB Systems with ISI," *IEEE Sarnoff Symposium*, pp.1-5, 2009.
- [24] R. Kshetrimayum, "An introduction to UWB communication systems," *IEEE Potentials*, Vol. 28, No. 2, pp.9-13, 2009.
- [25] G. Loubet and B. Faure, "Characterization of the underwater channel for acoustic communications", *Journal of the Acoustical Society of American*, Vol. 105, No. 2, pp. 1364, 1999.
- [26] Xiuzhen Cheng, Haining Shu, Qilian Liang and David Hung-Chang, "Silent Positioning in Underwater Acoustic Sensor Networks," *IEEE Transaction on Vehicular Technology*, Vol. 57, No. 3, pp.1756-1766, May 2008.